Photoconductive gain modelling of GaN photodetectors

1998 Semicond. Sci. Technol. 13 563

(http://iopscience.iop.org/0268-1242/13/6/005)

Semicond. Sci. Technol. **13** (1998) 563–568. Printed in the UK PII: S0268-1242(98)88751-8

Photoconductive gain modelling of GaN photodetectors

J A Garrido, E Monroy, I Izpura and E Muñoz

Dep. Ingeniería Electrónica, ETSI Telecomunicación, UPM, Ciudad Universitaria s/n, 28040 Madrid, Spain

Received 22 October 1997, in final form 5 January 1998, accepted for publication 6 February 1998

Abstract. A model to explain the behaviour of GaN photoconductive detectors is proposed, and it is based on the idea of a volume modulation rather than a carrier density modulation. Space charge regions inside the semiconductor produce a variation of the conductive volume when carriers are photogenerated. The strong non-exponential photocurrent decays result from carrier capture processes over the barriers associated with space charge regions. By means of computer simulation, this model explains quite well the behaviour of current GaN photoconductor devices and predicts their time response, temperature dependence and responsivity properties.

1. Introduction

GaN and related ternaries, AlGaN and InGaN, are promising materials for ultraviolet (UV) and visible optoelectronic devices because of their wide direct band gap. In addition, their ability to operate at extreme conditions of temperature and voltage bias makes them useful for transistors to be used in harsh environments. Because of their simplicity, photoconductive GaN detectors were intensively studied [1–5] during the initial developments of UV detectors. A classical photoconductive model that assumes a conductivity modulation (carrier density) owing to the photogenerated carriers was tentatively employed to explain the reported findings [6]. Although data published on GaN photodetectors usually differ owing to material quality-related issues, among the most significant characteristics the following have been found: (a) photocurrent response exists for photons with energies below the band gap, and usually photoconductive gains in the 10^3–10^4 range for photon energies above the band gap; (b) very slow non-exponential photoconductance decays; (c) a highly non-linear photocurrent response, depending on the illumination irradiance (P); (d) gain dependences on incident power, typically between $P^{-0.5}$ and $P^{-0.9}$, when a constant (DC) illumination or a chopped light source is used; (e) a significant dependence of the photoresponse with temperature.

Most of the above characteristics were initially linked to the existence of shallow and deep traps. The presence of bimolecular and monomolecular recombination regimes, controlled by states inside the band gap, has been claimed [2, 4, 7] to explain the reported non-linear responsivity behaviour in undoped layers, but a model explaining all the above features is still lacking.

Recently, we have proposed a model [8], based on the idea of a conductance modulation rather than a conductivity one. Space charge regions (SCRs) inside the semiconductor modify themselves as they separate photogenerated carriers. In this way the conductive volume inside the photoconductor is what actually varies, rather than the carrier density in 'fixed' volume. It is easy to show that this spatial modulation effect surpasses any carrier density increase effect owing to the photocarriers created, a result proven a long time ago by Hall measurements [9] and recently reported in frequency-resolved photoconductance studies [10].

Thermoionic theory has been used to account for the carrier trapping and detrapping over electrostatic barriers at the semiconductor boundaries. The strong non-exponential photocurrent decay results from a carrier capture process over a barrier, whose height increases with time while capture takes place. By means of computer simulation this model has been used to fit the behaviour of current GaN photoconductor devices and to analyse the measured time response dependences on temperature and incident optical power.

2. Gain model

2.1. Origin of the gain

Let us consider figure 1(a), where the charge density and the band diagram associated with a negatively charged semiconductor surface in the dark (broken line), and under illumination (full line) are shown. We want to point out that this band diagram, at least from the semiconductor side, is the same for a metal–semiconductor diode as for a naked semiconductor surface or intergrain interface. The presence

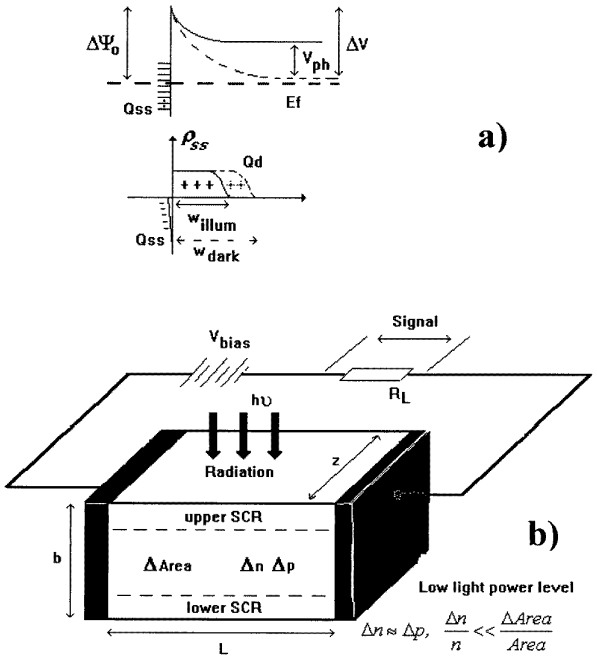

Figure 1. (*a*) Band diagram and charge density associated with a negatively charged semiconductor surface in the dark (– – –) and under illumination (——). (*b*) Experimental setup showing the air–semiconductor (upper) and the bulk–substrate (lower) SCRs.

of a high density of surface bound states for electrons, lying inside the gap and close to E_F, produces an E_F pinning effect. We will assume this situation in our model. Hence, the time evolution of the above surface SCR can be studied as the case of a Schottky diode on an n-type semiconductor under open-circuit conditions. Such a diode is a majority-carrier device (electrons) with a predictable behaviour both in the dark and under illumination, as well as during the switching transient. The surface charge density, Q_{SS}, owing to trapped or accumulated electrons is related to the surface band-bending, ΔV, by the expression

$$Q_{SS} = (2q\varepsilon N_d \Delta V)^{1/2} \approx (2q\varepsilon N_d \Delta\Psi_0)^{1/2} \qquad (1)$$

where q is the electron charge, ε is the permittivity of the material and $\Delta\Psi_0$ is the barrier height. We are assuming, for simplicity, a band-bending, ΔV, equal to the potential barrier, $\Delta\Psi_0$. The SCR width in the dark (w_{dark}) is given by the surface charge density, Q_{SS}, and the doping level (N_d) through the following expression:

$$w_{dark} = \left(\frac{2\varepsilon}{qN_d}\Delta\Psi_0\right)^{1/2}. \qquad (2)$$

When the sample is illuminated, the photoionized carriers are swept by the SCR and thus a variation in both Q_{SS} and the SCR width are produced, generating a photovoltage, V_{ph}. As a result a conductive volume increment is produced, because of the reduction of the SCR width from w_{dark} to w_{illum}, which is given by

$$w_{illum} = \left[\frac{2\varepsilon}{qN_d}(\Delta\Psi_0 - V_{ph})\right]^{1/2}. \qquad (3)$$

To understand the influence of this transverse photovoltaic effect in a photoconductor device, let us consider the configuration shown in figure 1(*b*), where a bulk sample is illuminated from the top surface. Associated with this surface there is an SCR (top surface) whose thickness varies with illumination, thus producing a variation of the conductive area (ΔArea). The bottom SCR (owing to the heterojunction with the buffer layer) also reacts if some carriers are photogenerated near it, as has been found experimentally in epitaxial GaAs layers [10]. For the sake of clarity, only the reaction of the upper SCR will be considered in this study. In addition to this volume variation (conductance modulation), one would expect a conductivity modulation owing to the increase of carrier densities (Δn, Δp). Nevertheless, simple calculations show that the first effect clearly dominates. As an example, for optical power densities of 100 W m^{-2} (corresponding to 10^{16} photons cm^{-2} s^{-1}), a typical value of the absorption coefficient ($\alpha = 10^4$ cm^{-1}) and GaN recombination lifetimes in the 10 ns range, only 10^{12} free carriers cm^{-3} would be generated in our sample. This variation (10 parts per million in our case with $n \approx 10^{17}$ cm^{-3}) cannot explain the large photoconductivity gains obtained under these conditions. It is clearly below the few parts per thousand of conduction volume variation that would take place in a sample with $b = 2$ μm, for example, if one uses equation (2) and equation (3), assuming $\varepsilon = 9.2$, a typical barrier height ($\Delta\Psi_0$) of 0.7 eV and only 100 mV of V_{ph}. The photoconductive gain (G) is defined as the increase in the number of collected carriers per absorbed photon (with an energy $h\nu$) and can be expressed as

$$G = \frac{\text{collected e}^-}{\text{absorbed photons}} = \frac{\Delta I/q}{P/h\nu} \qquad (4)$$

where ΔI is the measured current difference between dark and illumination conditions.

The usual sample conductivity formula applied to the sample of figure 1(*b*), assuming that $\Delta n/n \ll \Delta\text{Area}/\text{Area}$, and thus neglecting the effect of Δn, allows us to express the current increment as

$$\Delta I = \frac{\Delta\text{Area}}{L} q\mu n V_{bias} = \frac{z(w_{dark} - w_{illum})}{L} q\mu n V_{bias} \qquad (5)$$

where L is the sample length, z is its width, μ is the electron mobility and V_{bias} the applied bias voltage (as shown in figure 1(*b*)). Introducing this expression into the gain equation, equation (4), we obtain a full expression for the 'photoconductivity' gain:

$$G = \frac{h\nu}{q}\frac{I_{dark}}{b - w_{dark}} \times \frac{1}{P}\left\{\left(\frac{2\varepsilon\Delta\Psi_0}{qN_d}\right)^{1/2} - \left[\frac{2\varepsilon(\Delta\Psi_0 - V_{ph})}{qN_d}\right]^{1/2}\right\} \qquad (6)$$

where the dependences on L and with μ are included in the value of I_{dark} (for $V_{bias} = 5$ V, we have measured a dark current $I_{dark} = 2.5$ mA). Note that this gain comes from a geometrical (ΔArea) effect and not from carrier density variation. Therefore, in the following sections we will used the term photoconductance gain, since only the

sample conductance variations are really detected in the sample of figure 1(*b*). We will now describe in greater detail the device gain dependences under both DC and AC illumination conditions.

2.2. Dynamic behaviour

Let us consider again figure 1(*a*) as corresponding to a metal–semiconductor (n-type) Schottky diode. In the dark, two opposite electron fluxes exist over the barrier, namely thermionic emission from the metal towards the n-type semiconductor and a compensating flux (in mean value) from the semiconductor towards the metal. The second of the above electron fluxes can be seen as the electron current required to maintain the dynamic electron capture process at the surface or at interface states. As a first approximation we neglect the effect of the tunnelling currents. Therefore, to model the time evolution of the accumulated charge at the surface states, we take into account two competing processes, the electron thermionic emission from surface states ($J_{emiss} = AT^2 \exp(-\Delta\Psi_0/V_T)$) and the thermionic capture over the barrier of electrons from the bulk ($J_{cap} = AT^2 \exp\{[V_{ph}(t) - \Delta\Psi_0]/V_T\}$). The dynamic equation of the accumulated charge can be expressed as

$$\frac{\mathrm{d}Q_{SS}(t)}{\mathrm{d}t} = J_{cap} - J_{emiss} = AT^2\,\mathrm{e}^{-\Delta\Psi_0/V_T}(\mathrm{e}^{V_{ph}(t)/V_T} - 1) \tag{7}$$

where

$$V_{ph}(t) = \Delta\Psi_0 - \frac{Q_{SS}^2(t)}{2q\varepsilon N_d}. \tag{8}$$

To gain insight into the dynamic behaviour of this system, we will consider first the photoconductor recovery process after the switching-off of a light source that has been illuminating the top interface. Depending on the photon energy, the light source can create electron–hole pairs (photon energy above the band gap) that will be separated by the SCR, thus creating a photovoltage V_{ph}, but it can also ionize some interface traps even for photon energies below the band gap. In this case, the equilibrium surface charge (Q_{SS}) is affected (the number of trapped electrons is reduced), and this in turns requires a SCR shrinkage in order to make null the electric field in the bulk semiconductor region. In this way, a photoconductance response appears for photons with energy below the band gap. In both cases Q_{SS} is reduced and a photovoltage V_{ph} appears. Just after the light source is switched off, the capture flux surpasses the emission rate and an electron recapture process starts, governed by equation (7). This equation, solved numerically for the $V_{ph}(t)$ decay, leads to a very non-exponential behaviour, because as capture takes place $V_{ph}(t)$ decreases, thus increasing the capture barrier and lowering the capture rate. On the other hand, for the turn-on transient, the $V_{ph}(t)$ rise is much faster because of the much higher electron fluxes involved. This is also the experimental result for the turn-on transient conductance in GaN samples [8]. The wurtzite GaN samples used in this study were grown by MOVPE on sapphire substrates [11]. These GaN layers, with a thickness from 0.5 to 7 μm, were n type, nominally undoped, with an electron concentration (obtained by Hall measurements) in the 10^{16}–10^{18} cm^{-3} range. Concerning the strong non-exponential decay, figure 2 shows an experimental GaN conductance decay curve, measured at 300 K, together with a computer solution of equation (7). An He–Cd laser (325 nm) was used as the excitation source. A more detailed description of the experimental setup can be found elsewhere [8]. A barrier height of 0.684 eV, a doping level of 10^{17} cm^{-3} and $V_{ph} = 0.399$ V allow such good fitting. The semilogarithmic inset in figure 2 shows the strong non-exponentiality of the initial decay waveform. As indicated above, assuming only one barrier height we have obtained a good agreement between experimental data and the model theoretical predictions. An improved analysis can also be performed taking into account both the upper naked surface and the lower GaN–substrate interface.

Let us indicate an experimental consequence of this dynamic behaviour. While the stationary state corresponding to turning-on the illumination source is reached quickly (few seconds or minutes), the conductivity stationary state corresponding to the sample in the dark (turn-off), is a very slow process (hours or days of decay time). Thus we face a very non-linear system under AC light excitation, and some 'unexpected' results can be obtained when the sample photoresponse is measured using a 50% time-on 50% time-off chopped light source, as we will show below.

2.3. Gain dependence on optical power

Once the photoconductance gain mechanism in GaN has been described, one needs to relate the impinging photon flux to the photovoltage developed in the SCR. For photons with energy above the band gap, one can assume that all the generated electron–hole pairs are separated by the SCR (or at least this holds for those being generated within a diffusion length [12]). If this was not the case, an efficiency factor could be taken into account in the quantum efficiency η. In the steady state, the surface band-bending has been reduced by an amount V_{ph} that allows an electron flux to reach the surface equal to the hole one arriving by drift and equal to the electron–hole pairs photogenerated per second and unit area in the sample. Taking these fluxes into account, one can evaluate the SCR width variation for a given optical power or, in other words, the photoconductance gain for a given optical power can be calculated. Therefore, under constant illumination, a photovoltage will appear when $J_{emiss} = J_{cap}$. In this way the well-known Schottky diode photovoltage equation can be used:

$$V_{ph} = V_T \ln\left[1 + \mathrm{e}^{\Delta\Psi_0/V_T}\left(q\eta\frac{P}{h\nu AT^2}\right)\right]. \tag{9}$$

Introducing equation (9) into equation (6), the desired gain–optical power relation is obtained for different temperatures. Because of the logarithmic dependence of V_{ph} on the optical power, one can foresee a strong gain compression in spite of the square root dependence of $\Delta\Psi_0$ in equation (6). This is seen in figure 3, especially at

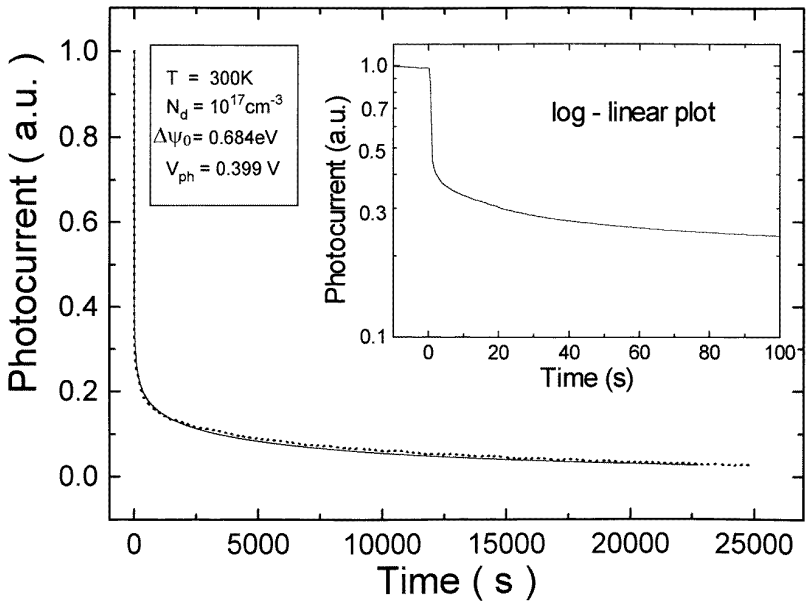

Figure 2. Photoresponse decay of a GaN detector after an He–Cd laser light pulse (λ = 325 nm) of 4.6 mW m^{-2}. The experimental non-exponential law (·····) is fitted by the simulation results (——). The semilogarithmic plot of the inset shows the very non-exponential initial temporal response.

not too high temperatures, where the gain versus optical power follows an inverse power law ($G \propto P^{-K}$), with K increasing as temperature decreases. The flat gain region that appears at extremely low powers and high temperatures is due to low V_{ph} values developed in the SCR, when the number of carriers swept per second by the SCR is low compared with the thermionic electron fluxes over the barrier. This is equivalent to a linearization of equations (9) and (6), the latter because of a small SCR width variation compared with the SCR width itself. In this case the system is linear (constant gain versus power), while the regions having $G \propto P^{-1}$ remind us that in a Schottky barrier its dynamic resistance is inversely proportional to the bias current, a behaviour clearly observed in the frequency domain for GaAs photoresistors [10, 13]. Concerning experimental results in GaN samples, it is worth mentioning that the huge values of the photoconductance gain predicted by the model agree with the experimental results [8]. Moreover, for low–medium temperatures and medium–high powers, a linear P^{-K} dependence, with K close to 0.9, has been reported by Muñoz *et al* [8] and, as the temperature is increased, the K exponent is reduced. The predicted saturation region at low optical powers was not experimentally found by Muñoz *et al* [8], but it has been reported by Binet *et al* [4].

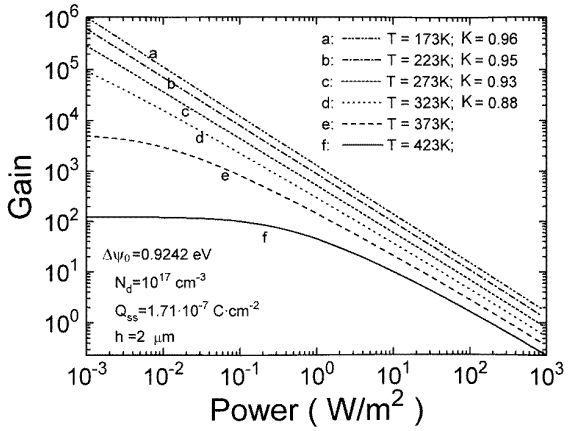

Figure 3. Computer simulations of the DC photoconductor gain versus irradiance and temperature, coming from the proposed conductive volume modulation mechanism. A decrease of the K exponent with increasing temperature and the appearance of a flat gain region at very low optical power ranges are predicted by the model.

2.4. DC gain versus AC gain

The theoretical gain–optical power dependences presented in figure 3 ($G \propto P^{-K}$) correspond to DC gain measurements. However, for low-level power measurements a common way to reduce noise is to use a chopped light source and a synchronous detection system. Using this setup, the AC photoconductance gain was also studied by means of a frequency-programmable chopper and a lock-in amplifier. More details about the experimental setup can be found in [8]. As a general trend, the P^{-K} dependence has also been found, with K decreasing as the chopper frequency is increased. As an example, the K exponent decreases from 0.65 to a value of 0.55 when the chopper frequency changes from 66 Hz to 135 Hz. These K values, closer to 0.5 than to 1, are consistent with the experimental data reported by Binet *et al* [4]. As will be shown, the measured AC gain dependences (with optical power and modulation frequency) agree with our model predictions.

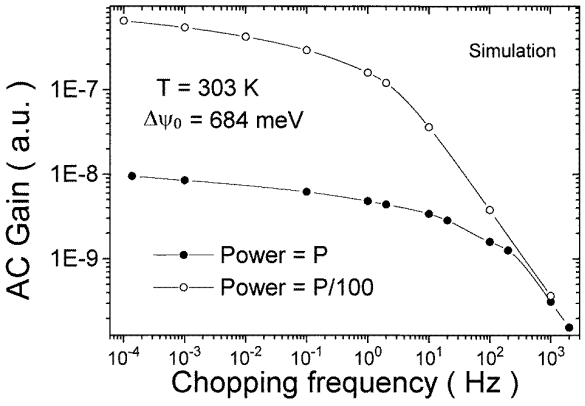

Figure 4. Simulation results of the AC gain versus chopping frequency for two different exciting optical powers.

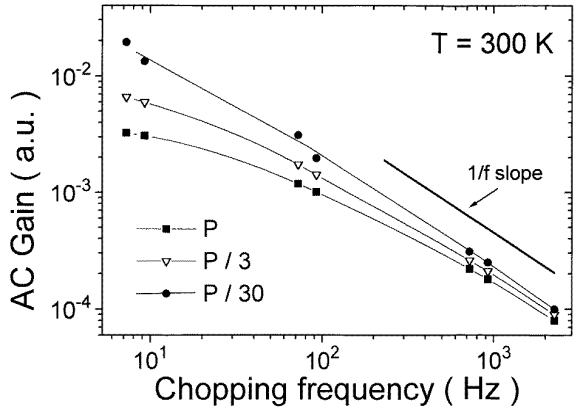

Figure 5. Experimental AC gain versus chopping frequency measured for three different optical powers. The chopping frequency range is limited by the experimental system. In spite of the limited frequency range shown with that of figure 4, the same trends are observed: a flat region at low frequencies and a $1/f$ region at high frequencies are present.

Figure 4 represents the theoretical AC gain versus the chopping frequency for two optical powers (P and $P/100$). While a region of constant gain is observed at low frequencies, an inverse frequency dependence law ($1/f$) appears at high frequencies, where all the curves merge into a single one. Separating the two regions, there is a corner frequency that increases with power, indicating that the photoconductor shows a kind of 'gain–bandwidth product' conservation law. At low enough frequencies, a quasi-DC regime, with $G \propto P^{-0.9}$, can be observed. When extremely low optical powers are used, a deviation of the P^{-K} law is expected, which has recently been observed by Kung *et al* [5] and Goldenberg *et al* [14]. As the chopping frequency increases, the K exponent decreases (smaller separation between curves). This would explain the K values close to 0.5 reported in [4]. In this frequency range the generated photovoltage becomes nearly constant, with small triangle-like swings proportional to the excitation period ($1/f$ law) rather than to the incident optical power, as is shown below.

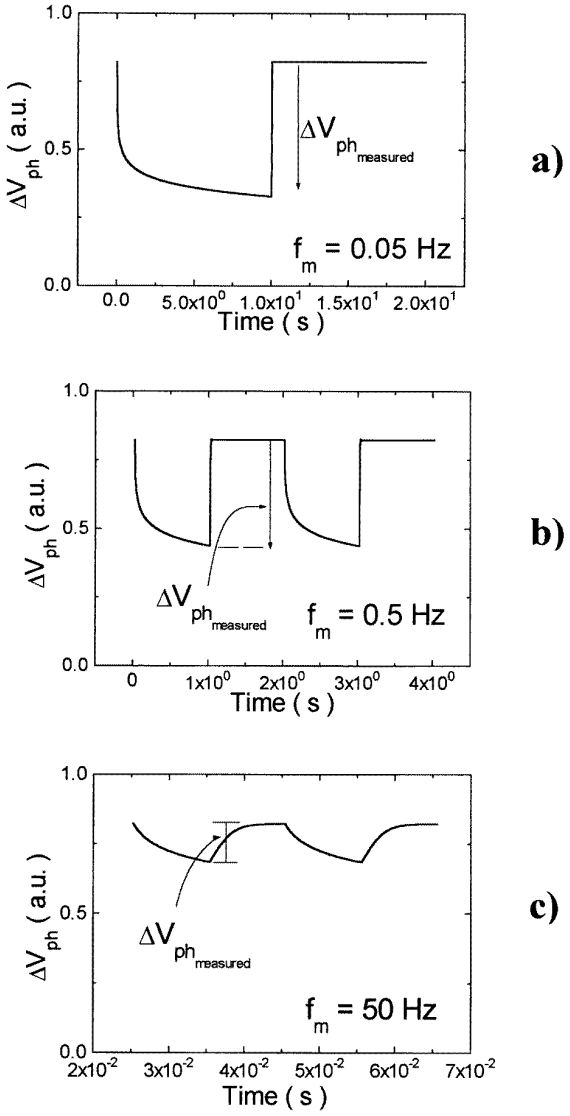

Figure 6. Simulated photovoltage decay and build-up cycles of the GaN photoresponse for AC excitation using T = 303 K and $\Delta\Psi_0$ = 684 meV. As the chopping frequency is increased, the measured ΔV_{ph} is decreased, and the waveform becomes more symmetric, approaching a triangular waveform at high frequencies.

Figure 5 shows the experimental dependence of the AC gain on the chopping frequency, for different optical powers, in a GaN photoconductor. These results, in agreement with the predictions of figure 4, confirm the validity of the proposed model, and indicate the importance of a proper selection of the working frequency. To understand how the AC gain becomes proportional to the excitation period ($1/f$ region), figure 6 shows the simulated photovoltage waveforms generated in an SCR being illuminated by the same optical power, but chopped at different frequencies. At $f_m = 0.05$ Hz, the $\Delta V_{ph}(t)$ dark to illumination transient seems to be instantaneous, while a strong non-exponential $\Delta V_{ph}(t)$ decay (on to off) lasts for much more time, and the peak $\Delta V_{ph}(t)$ is about

60% of the maximum V_{ph}. At $f_m = 0.5$ Hz, the turn-on transient still looks very fast, but the $\Delta V_{ph}(t)$ decay cannot reach the same low level reached at 0.05 Hz, giving a lower ΔV_{ph} swing, a lower SCR width variation and thus a lower AC gain. Finally, at 50 Hz, both the turn-on and the turn-off $\Delta V_{ph}(t)$ transients look slow, and the ΔV_{ph} excursion is rather small. In fact we would now be entering the $1/f$ frequency-dependent AC gain region (see figure 4). The true $1/f$ region is reached when the chopper frequency is high enough for ΔV_{ph} to have a triangular wave shape, and thus the photovoltage swing ΔV_{ph} is proportional to the excitation period.

3. Conclusions

GaN and AlGaN photoconductors are devices of interest as UV detectors. A new model, based on a modulation mechanism of the conductive volume of GaN photoconductors, able to explain their huge photoconductive gain values and dependences experimentally found has been presented. SCRs and their associated potential barriers, generated by charge accumulation at free surfaces or bulk dislocations, produce a spatial separation of the photogenerated carriers. The capture processes, explained by means of a thermionic theory, are controlled by such potential barriers and lead to a very slow and non-exponential recovery process. A complete study of the photoconductor gain dependences on power, temperature and frequency has also been performed. All the remaining features experimentally found, such as the highly non-linear response as well as the P^{-K} gain dependence, with K ranging from 0.9 to 0.5, are predicted by the model as well as the strong gain dependence on temperature. The differences previously reported for AC and DC gain measurements can also be easily understood from present model.

Acknowledgments

This work was partially supported by Plan Futures 1996-9 Contract TECN-96-1054, by CICYT TIC95-0116 and TIC95-0770 projects, and by Comunidad de Madrid project 06M-019-96.

References

[1] Khan M A, Kuznia J N, Olson D T, Van Hove J M and Blasingame M 1992 *Appl. Phys. Lett.* **60** 2917
[2] Stevens K S, Kinniburgh M and Beresford R 1995 *Appl. Phys. Lett.* **66** 3518
[3] Walker D, Zhang X, Kung P, Saxler A, Javadpour S, Xu J and Razeghi M 1996 *Appl. Phys. Lett.* **68** 2100
[4] Binet F, Duboz J Y, Rosencher E, Scholz F and Härle V 1996 *Appl. Phys. Lett.* **69** 1202
[5] Kung P, Zhang X, Walker D, Saxler A, Piotrowski J, Rogalski A and Razeghi M 1995 *Appl. Phys. Lett.* **67** 3792
[6] Sze S M 1981 *Physics of Semiconductor Devices* 2nd edn (New York: Wiley)
[7] Qiu C H, Melton W, Leksono M W, Pankove J Y, Keller B P and Denbaars S P 1996 *Appl. Phys. Lett.* **69** 1282
[8] Muñoz E, Monroy E, Garrido J A, Izpura I, Sánchez F J, Sánchez-García M A, Calleja E, Beaumont B and Gibart P 1997 *Appl. Phys. Lett.* **71** 870
[9] Queisser H J and Theodorou D E 1979 *Phys. Rev. Lett.* **43** 401
[10] Izpura I, Valtueña J F and Muñoz E 1997 *Semicond. Sci. Technol.* **12** 678
[11] Beaumont B, Vaille M, Boufaden T, El Jani B and Gibart P 1997 *J. Crystal Growth* **170** 316
[12] Aldao C M, Valtueña J F, Izpura I and Muñoz E 1994 *Phys. Rev.* B **50** 17 729
[13] Vilcot J P, Vaterkowski J L and Decoster D 1984 *Electron. Lett.* **20** 87
[14] Goldenberg B, Zook J D and Ulmer R J 1995 *Topical Workshop on III–V Nitrides Proc.* (Nagoya: North-Holland)